

Absence of bones in archaeological sites from the southeast of Uruguay: Taphonomy or human behavior?

Ximena S. Villagran¹  | Mauricio Rodriguez²  | Heinkel Bentos Pereira²  |
 Camila Gianotti^{2,3}  | Moira Sotelo³  | Laura del Puerto² 

¹Museu de Arqueologia e Etnologia,
 Universidade de São Paulo, São Paulo, Brazil

²Centro Universitario Regional del Este,
 Universidad de la República, Rocha, Uruguay

³Laboratorio de Arqueología del Paisaje y
 Patrimonio del Uruguay, Facultad de
 Humanidades y Ciencias de la Educación,
 Universidad de la República, Montevideo,
 Uruguay

Correspondence

Ximena S. Villagran, Museu de Arqueologia e
 Etnologia, Universidade de São Paulo, São
 Paulo, Brazil.

Email: villagran@usp.br

Funding information

Fundação de Amparo à Pesquisa do Estado de
 São Paulo (FAPESP), Grant/Award Number:
 2015/19405-6; Comisión Sectorial de
 Investigación Científica (CSIC I+D),
 Grant/Award Numbers: 2017-2019/338,
 2015-2017/94

Abstract

The rework of daily refuse, including large quantities of faunal remains, is a common explanation for earthen mound construction in the Uruguayan lowlands, which started about 5000 years ago. While some earthen mounds contain human and animal bones in high abundance, several others contain only a few fragments. Thousands of years later (17th to 18th centuries), stone structures known as cairns were used in the same region and are believed to have served as the burial ground for local chiefs. However, no bone remains were ever found during excavations. The acidity of local soils has been the common explanation for the low frequency and/or complete absence of bone remains in earthen mounds and cairns. To investigate the absence of bones possibly induced by a corrosive environment, we applied Fourier transform infrared spectroscopy (FTIR), X-ray powder diffraction (XRPD), and micromorphology to study the sediments at three sites: (1) an earthen mound rich in macroscopic bone fragments (CH2D01 site—CH); (2) an earthen mound with only a few macroscopic bone fragments (Las Palmas—LP); and (3) sediments from beneath a cairn with no macroscopic bone remains (Mario Chafalote cairn—MC). FTIR and XRPD showed the existence of burnt bones at the CH mound and a complete absence of bone mineral at LP and MC. Micromorphology revealed that, though invisible in the FTIR spectra, the LP mound contains micro-bone fragments, but in extremely low frequency. Analyses indicate that taphonomy did not play a major role in the low frequency or absence of bones at the LP and MC sites, located in a similar environmental context, and that differences in site use and mound technology explain the contrasting composition of the CH mound.

KEY WORDS

cerritos, FTIR, geoarchaeology, micromorphology, XRPD

1 | INTRODUCTION

Animal bones are indispensable sources of data for inferring past subsistence and foraging activities, and their taphonomic study reveals fundamental information about the weathering processes

affecting archaeological deposits. Determining their presence or absence has great implications for the interpretation of site formation processes and the human activities at a specific site. The absence of bones in an archaeological site leads to two kinds of interpretations: one related to human behavior (i.e., bones were never deposited) and

another related to diagenesis (i.e., bones were present in the past, but dissolved due to local burial conditions).

The type and the intensity of postdepositional processes that affect bone remains in archaeological sediments depend on the degree of burning, and local burial and environmental factors (e.g., the sedimentary context, rain regime, pH, groundwater, microbial attack, etc.) (Berna et al., 2004; Collins et al., 2002; Dal Sasso et al., 2016; Hedges, 2002; Jans, 2004; Karkanas, 2010; Nielsen-Marsh & Hedges, 2000; Nielsen-Marsh et al., 2007; Smith et al., 2007; Trueman et al., 2004; Weiner, 2010). Collagen loss, dissolution, and recrystallization of the bone mineral, commonly defined as bioapatite or carbonate hydroxyapatite $[\text{Ca}_5(\text{PO}_4)_3(\text{OH})]$ (LeGeros & LeGeros, 1984; Skinner, 2005), are the most usual diagenetic pathways.

In the southeast of Uruguay, indigenous constructions, such as earthen mounds and cairns, are the most prominent features of the archaeological landscape. Earthen mounds, locally known as *Cerritos de Indios*, are widespread in the north and southeast of Uruguay and the south of Brazil from ca. 5000 B.P. to the 17th–18th centuries (Bracco, 2006; Bracco et al., 2015; Cabrera, 2005; Gianotti, 2005; Lopez-Mazz, 2001). Earthen mounds are formed by a complex combination of uses and activities, including intentional construction episodes, unintentional sediment accumulation produced by domestic settlements, phases of abandonment and reoccupation, human burials, and maize cultivation. (Bracco, 2006; Cabrera, 2005; Femenias et al., 1990; Gianotti & Lopez-Mazz, 2009; Iriarte, 2006; Moreno, 2017; Villagran & Gianotti, 2013). As part of these dynamics, domestic waste, mostly consisting of bone remains, charcoal, lithic debris, and pottery sherds, may become integrated to the sedimentary matrices.

Cairns are human-made stone arrangements in the shape of small circles or piled up to create small mounds. They are commonly located on the top of prominent hills, in places with good visibility. They are described in chronicles from the 17th to 19th centuries as points of observation or territorial control, as the location of hearths that produce fire signals or as markers signaling the location of indigenous tombs (Femenias, 1983; Figueira, 1958; Sotelo, 2018). Both earthen mounds and cairns are believed to contain bones, and their absence has been commonly attributed to soil acidity (Capdepont et al., 2005; Capdepont & Pintos, 2006; Pintos & Capdepont, 2001).

In open-air contexts, the direct exposure to environmental factors and, often, low pH increase the alteration and final destruction of bones. Berna et al. (2004) showed that bone mineral is well preserved at pH above 8, dissolves and recrystallizes at pH between 8.1 and 7.4, and dissolves and bonds with Al or Mg at pH below 7. Thus, in the absence of alkaline material, the expected situation in open-air contexts is that of intense dissolution of the bone mineral. In our study area, soil pH varies from 4.8 to 6.9, favoring the dissolution and bonding of bone mineral with Al or Mg. However, if bones were present in the soil, traces of their existence could be detected by the identification of carbonate hydroxyapatite or other phosphate minerals associated with bone dissolution and recrystallization, such as

montgomeryite or francolite (also termed carbonate fluorapatite). These minerals have been identified in archaeological sediments mostly by Fourier transform infrared spectroscopy (FTIR), sometimes combined with other techniques such as X-ray fluorescence and X-ray diffractometry (Friesem et al., 2016; Karkanas, 2000; C. E. Miller et al., 2013; Nriagu et al., 1976; Schiegl, 1996; Stiner et al., 2001; Weiner, 2010; Weiner et al., 1995, 2002).

FTIR is frequently used in archaeological science to study the mineral replacement and recrystallization processes that take place in both weathered and heated bones (Berna et al., 2004; Dal Sasso et al., 2016; Lebon et al., 2010; Shahack-Gross et al., 1997; Snoeck et al., 2014; Squires et al., 2011; Stiner, Khun, Bar-Yosef, et al., 1995; Stiner et al., 2001; Stiner, Khun, Weiner, et al., 1995; Thompson et al., 2009; Toffolo et al., 2015; Trueman et al., 2004; Weiner & Bar-Yosef, 1990). FTIR is an inexpensive, easy to use technique that allows rapid analysis of large sets of samples (Monnier, 2018; Weiner, 2010; Weiner & Bar-Yosef, 1990).

Here, we report the results of a geoarchaeological study of two earthen mounds and a cairn from southeastern Uruguay using FTIR spectroscopy, X-ray powder diffraction (XRPD), and micro-morphology. The FTIR spectra were analyzed using the second derivative for better identification of the phosphate bands. We focused on the spectral range between 700 and 500 cm^{-1} , where phosphate bands can be readily isolated from clay using the second derivative. To validate the FTIR results, XRPD measurements were performed in selected samples and the results were contrasted with micro-morphological observations. To group all sets of samples according to their FTIR spectra, and extract statistically significant information from high-dimensional data, both the absorbance and second derivative spectra were processed by multiple component analyses (principal component analysis [PCA]).

2 | MATERIALS AND METHODS

2.1 | Archaeological samples

Samples for this study came from three indigenous constructions located in the southeast of Uruguay (Figure 1a): two earthen mounds (Figure 1b,c) and one cairn (Figure 1d). The CH2D01 site (CH) is an earthen mound site formed by two mounds (A and B) about 1.3 m high and 35 m long. Both mounds were built between 2755 and 2426 cal B.P. (93.8% probability; URU022) and 232–124 cal B.P. (37.5% probability; URU014) (Bracco et al., 2000; Curbelo et al., 1990) (Figures 1b and 2). Human remains were recovered from both mounds, with 21 individuals in mound A, and six individuals in mound B (Moreno et al., 2014; Portas & Sans, 1995; Sans & Femenias, 2000). Bones are present in almost every layer of the site, and zooarchaeological studies indicated that the wide majority corresponds to fish, followed by deer (*Ozotoceros bezoarticus*) and guinea-pigs (*Cavia aperea*), among other species (Bica, 2020; Moreno, 2014, 2016; Pintos, 2000; Pintos & Gianotti, 1995).

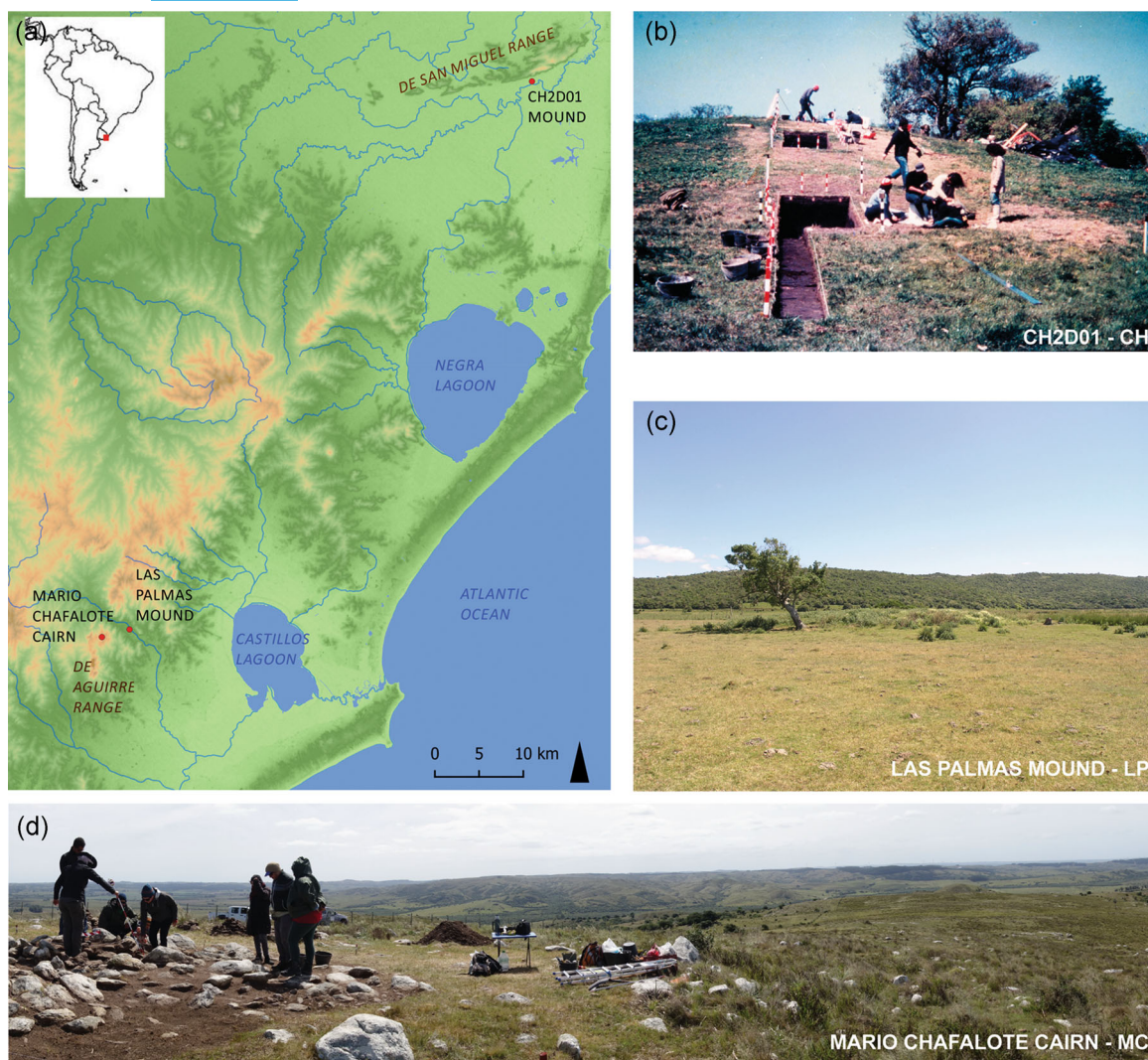


FIGURE 1 (a) Map of eastern Uruguay with the location of the three archaeological sites analyzed in this study: CH2D01 mound (CH), Las Palmas mound (LP), and Mario Chafalote cairn (MC); (b) CH site excavations in the 1990s (photograph by José López-Mazz); (c) View of the LP mound with de Aguirre mountain range in the background; and (d) view of the MC cairn located on top of the Aguirre range [Color figure can be viewed at wileyonlinelibrary.com]

The Las Palmas site (LP) is an earthen mound also consisting of two mounds (1 and 2) (Figures 1c and 2). Mound 1 is 35 m long and 1 m high, and mound 2 is 28 m long and 0.5 m high. Few heated and calcined bone fragments were recovered after wet sieving of the archaeological sediments. The first episode of mound construction took place at 2965–2859 cal B.P. (95% probability; Beta458464) and the second at 2745–2680 cal B.P. (95% probability; Beta442080) (the third and last episode has not yet been radiocarbon dated).

The Mario Chafalote (MC) cairn (Figures 1d and 2) was abandoned by the time of the European colonization (540–497 cal B.P., 95.4% probability, CNA4079-1; 315–267 cal B.P., 44.7% probability; Beta442081) and provided the first radiocarbon chronology for the Uruguayan cairns. The MC cairn is a structure 7 m in length, with a maximum height of 0.68 m. Besides numerous quartz flakes, only a polished lithic artifact (locally known as *boleadora*) was recovered, a type of artifact described in the chronicles as being commonly found

next to indigenous human interments (Figueira, 1965). However, no human remains were recovered from the site, weakening the hypothesis of its use as burial ground.

The archaeological samples from CH and LP were collected from the stratigraphic profiles at 5 cm intervals. The samples from CH were taken from mound B, sector IB (excavation III). Samples from LP were taken from the stratigraphic profile of mound 1 (east profile). Sediment samples from MC were collected from different locations at shallow depths beneath the stone pile at the center of the site (Figure 2). All archaeological samples were analyzed by FTIR and a selection was also measured by XRPD. For micromorphological analyses, two undisturbed block samples were collected from MC (Figures 2 and 6a) and four blocks were collected from LP (Figures 2 and 5a). No samples for micromorphology are available for CH because excavations at this site were concluded in the 1990s.

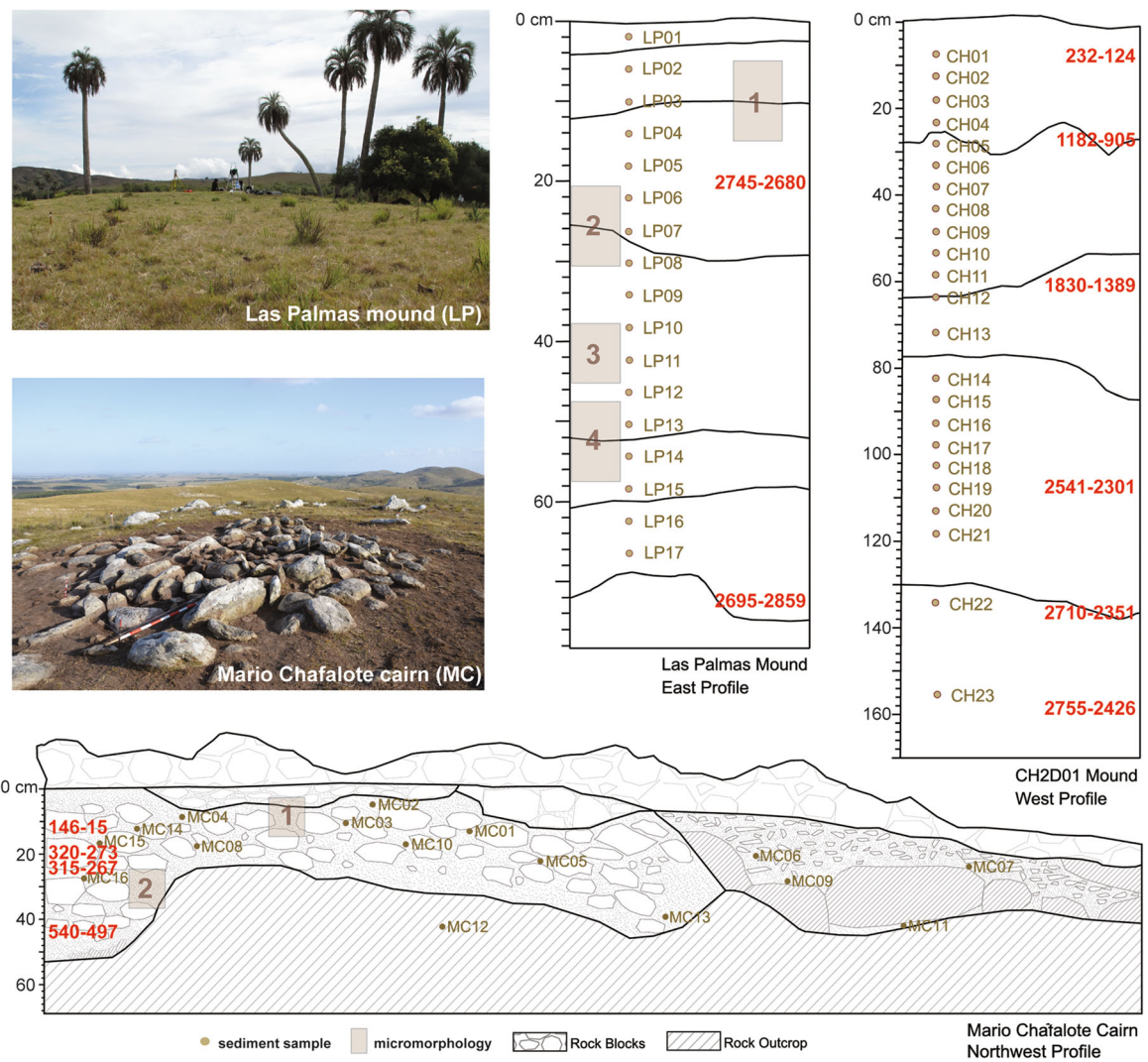


FIGURE 2 Archaeological sites used for this study. Las Palmas mound (photo); CH2D01 mound; and Mario Chafalote cairn (photo). Schematic view of the stratigraphic profiles with the location of the sediment and micromorphology samples used for this study. Calibrated ages are in years B.P. (red captions) [Color figure can be viewed at wileyonlinelibrary.com]

TABLE 1 List of archaeological and reference samples used in this study

	Quantity	Description
Archaeological samples		
CH	23	CH2D01-B mound, profile samples
LP	17	Las Palmas mound, profile samples
MC	16	Mario Chafalote cairn, excavation samples
Reference samples		
SOIL1	1	Local soil material from the A horizon near MC site
SOIL2	1	Local soil material from the A horizon near MC site
HB-A	1	Human humerus from the India Muerta site (Rocha, Uruguay)
HB-B	1	Human maxilla from the India Muerta site (Rocha, Uruguay)

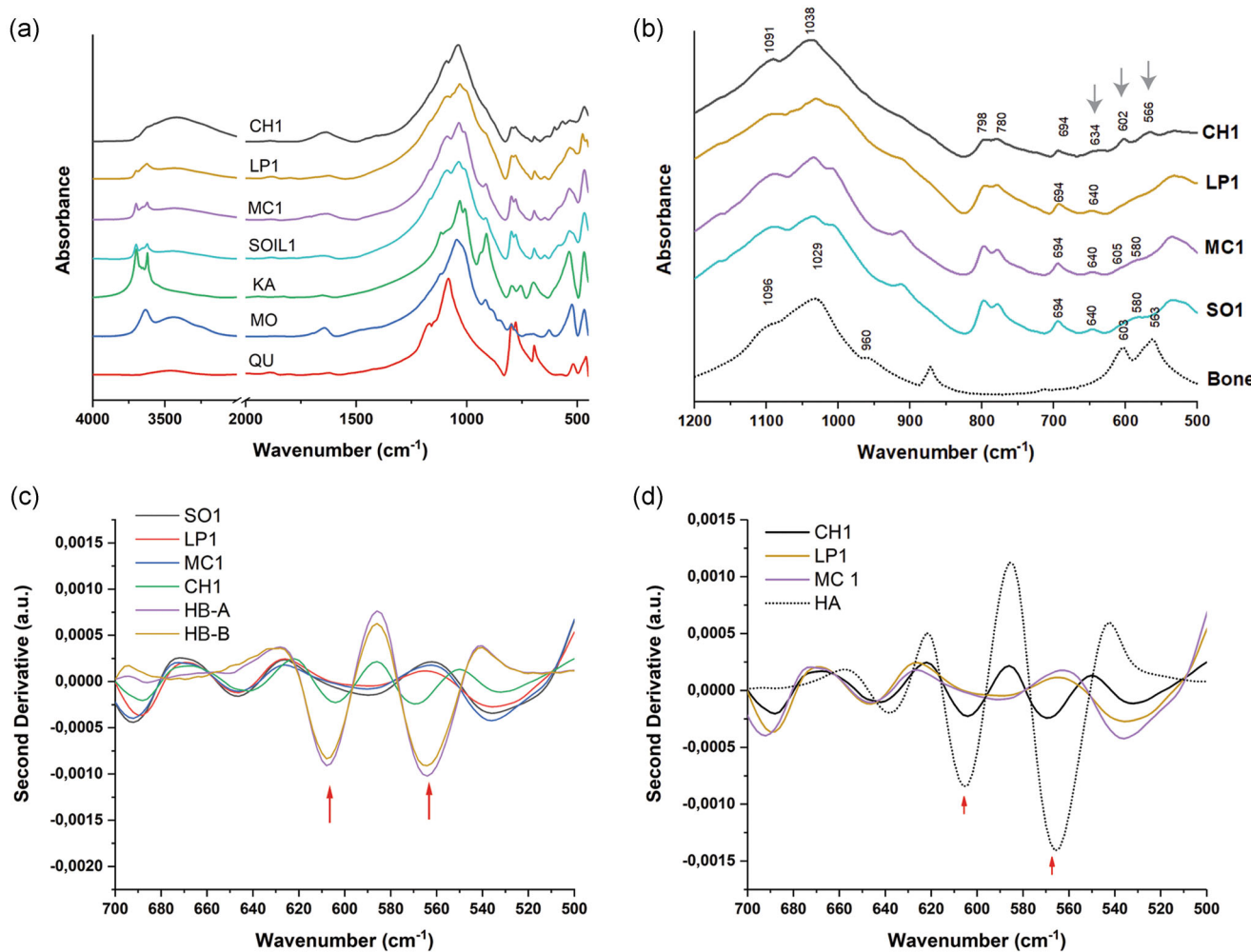


FIGURE 3 (a) Fourier transform infrared spectroscopy (FTIR) spectra of representative samples from CH, LP, and MC, with reference spectra from local soils (SOIL1) and several reference minerals present in the samples (QU = quartz; KA = kaolinite; MO = montmorillonite) (the complete spectra from CH, LP, MC, and reference soils are available as the Supporting Information Material). (b) Details of the FTIR spectra between 1200 and 500 cm⁻¹ of archaeological and reference samples from local soils and bone with an indication of peak values. Only samples from CH show the 602 and 566 cm⁻¹ $\nu_4\text{PO}_4$ phosphate components in the FTIR absorbance spectra. (c) Second derivative spectra of three representative archaeological samples from CH, LP, and MC, one sample of the reference soil, and two samples of human bone (HB). The two arrows indicate the locations of the $\nu_4\text{PO}_4$ phosphate components (at 604 and 565 cm⁻¹) of carbonate hydroxyapatite in the bones. See the almost perfect match between LP, MC and the reference soil and the two phospha components in the CH sample. (d) Second derivative spectra of three representative archaeological samples from CH, LP, MC, and one sample of hydroxyapatite from Sigma-Aldrich. Only the sample from CH demonstrates the presence of hydroxyapatite. Two minima are also observable in the MC and LP samples at lower wavenumbers, which cannot be assigned to the $\nu_4\text{PO}_4$ vibrational modes. CH, CH2D01 mound; LP, Las Palmas mound; MC, Mario Chafalote cairn [Color figure can be viewed at wileyonlinelibrary.com]

Off-site reference samples from the surface horizon near the MC site were measured to serve as control spectra for the archaeological samples (Table 1).

2.2 | FTIR

Archaeological and reference samples were measured by FTIR spectroscopy using a Perkin Elmer Frontier spectrophotometer.

Measurements were performed at room temperature between 4000 and 450 cm⁻¹ with a resolution of 2 cm⁻¹ (60 scans per sample). Samples were ground using a ball mill (Across international) to micro-size particles, homogenized in an agate mortar, and left to dry overnight. FTIR analyses were performed using KBr pellets. Diluted samples (0.25% wt) were homogenized in an agate mortar for 1 min. Samples mixed with KBr were pressed using vacuum pressure at 10 Ton. The transparent pellets (13 mm) obtained from this process were immediately measured in triplicate. All spectra were collected in

absorbance mode, and background correction was performed before measurements using Perkin Elmer software.

The second derivative of the FTIR spectra is commonly applied to analyze complex spectra with overlapping bands and to identify the position of weak peaks that appear as shoulders in the raw spectra (Aragão & Messaddeq, 2008; Lebon et al., 2008). We used the second derivative to highlight the underlying bands in the spectral region between 700 and 500 cm⁻¹, where the two antisymmetric bending phosphate bands ($\nu_4\text{PO}_4$) at 656 and 605 cm⁻¹ can be present in sediments containing carbonate hydroxyapatite. This is a complex region in our samples, given the multiple overlapping peaks corresponding to clay minerals, quartz, and bone mineral (the stretching vibrations of the carbonate and phosphate groups). Second derivative spectra were calculated from the absorbance spectra and after smoothing using 10-point Savitzky-Golay algorithms. All calculations were performed using Origin Pro software (OriginLab).

2.3 | XRPD

A selection of archaeological samples from CH (samples 2, 3, 4, 7, 9, 11, 16, and 20), LP (samples 1, 4, 8, 12, and 15), MC (samples 1, 4, 8, 12, and 16), and reference bone samples (HB) were analyzed by XRPD. Samples were grounded in an agate mortar to less than 25 μm and analyzed with PANalytical X'Pert equipment using Bragg Brentano configuration and a linear detector. Data were collected between the range 5 and 90° with a 0.02° step for all samples. The precision of the instrument was confirmed using NIST standard reference material 640d (< 1% precision). Highscore software (PANalytical) was used to compare the data with the PDF-2 (ICDD) and the COD databases.

2.4 | Micromorphology

Samples for micromorphological analyses were collected only from the stratigraphic profiles of LP and MC sites (Figures 2, 5a, and 6a). No samples from CH sites were available for this study because the site no longer exists. Blocks were impregnated with a mixture of polyester resin, styrene, and a catalyst and sliced into 7.5 \times 5 cm and 30- μm -thick thin sections. Samples were analyzed using a Leica S9i stereomicroscope and a Leica 2700P petrographic microscope under plane-polarized light and cross-polarized light at magnifications ranging from $\times 25$ to $\times 200$. Micromorphological descriptions followed the guidelines of Stoops (2003).

2.5 | Statistical analyses

The results of the FTIR measurements were grouped and classified by PCA using Origin Pro Software (OriginLab). The correlation matrix of a spectrum contains hundreds to thousands of values, depending on

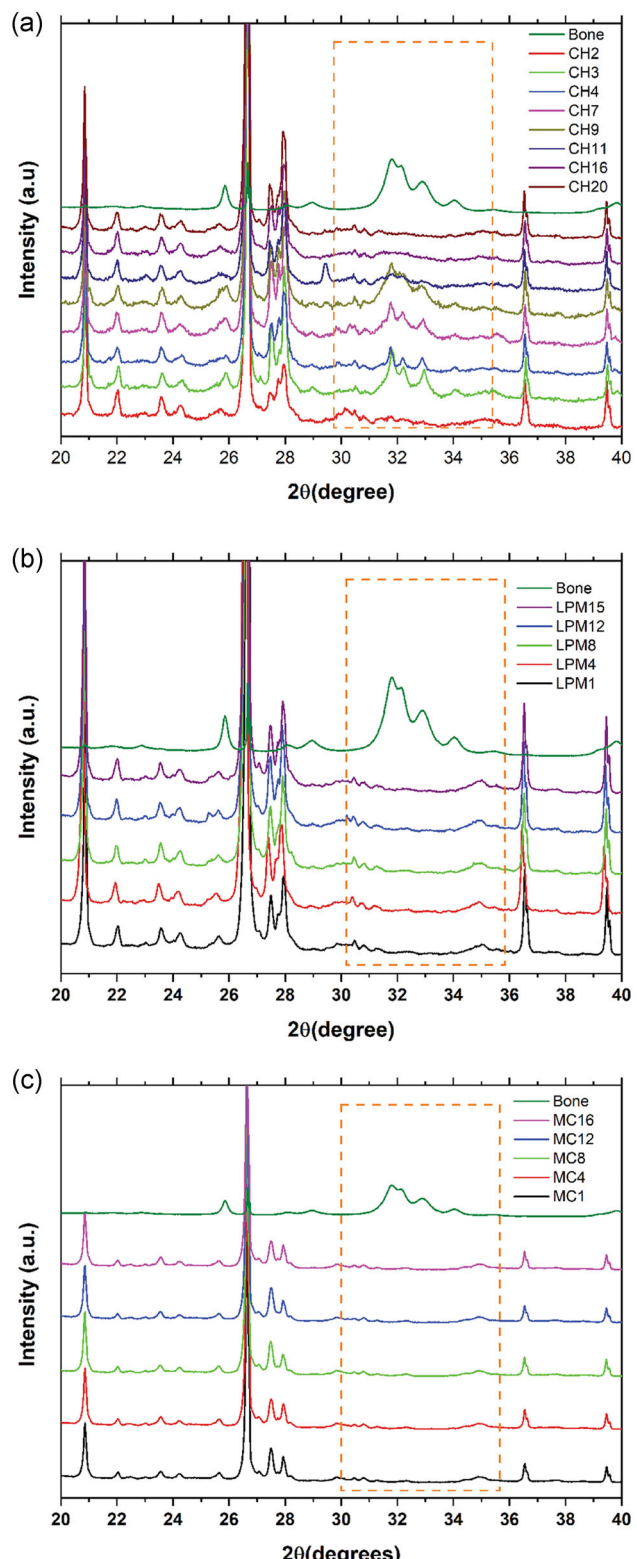


FIGURE 4 (a) Diffractograms of eight samples from the CH site and bone mineral; (b) diffractograms of five samples from the LP site and bone mineral; and (c) diffractograms of five samples from the MC site and bone mineral. The intensity of the plots was adjusted for better visualization. CH, CH2D01; LP, Las Palmas; MC, Mario Chafalote [Color figure can be viewed at wileyonlinelibrary.com]

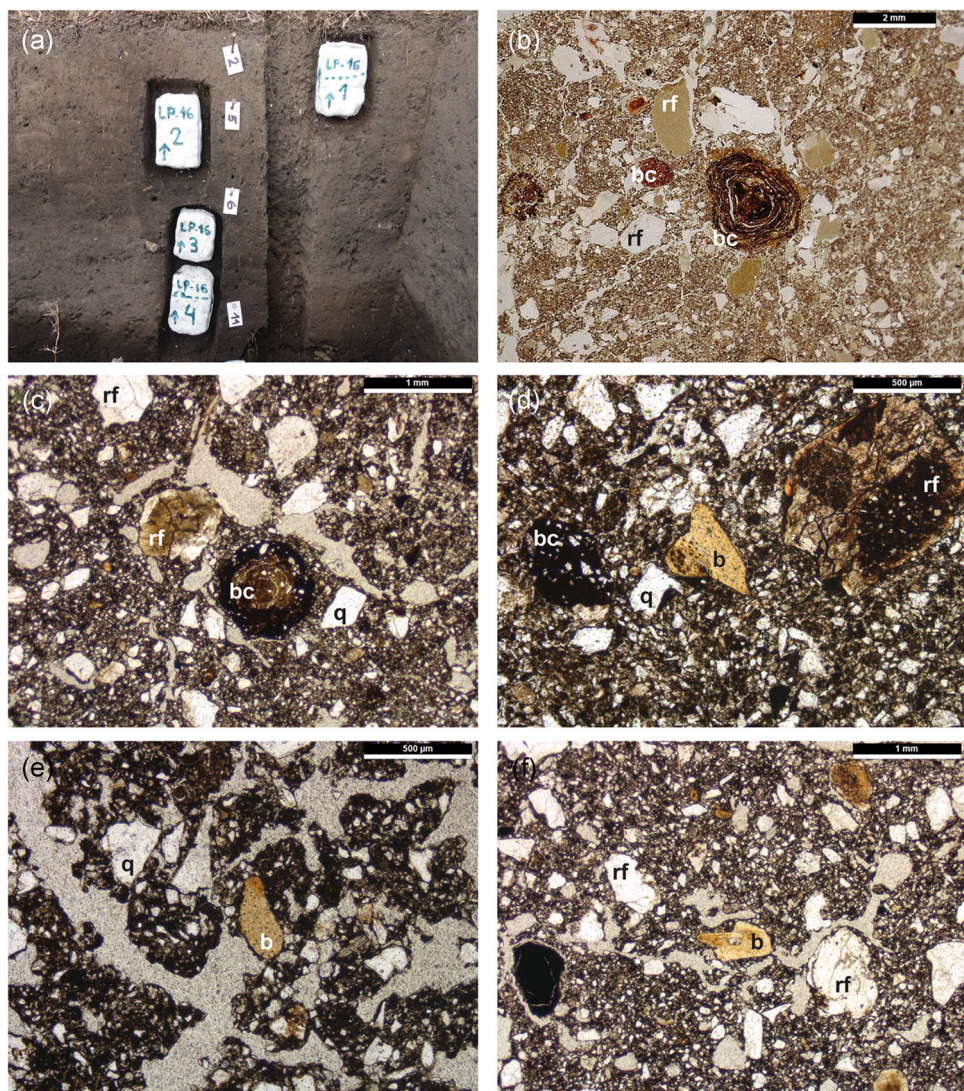


FIGURE 5 Micromorphology from the LP site. (a) Profile of the Las Palmas mound (LP) with the location of the four blocks for micromorphology; (b) sample LP-15-1 with burnt clay aggregates (bc) and rock fragments (rf) (PPL); (c) photomicrograph of sample LP-15-4 with burnt clay aggregate (bc) in the dark brown organomineral matrix (PPL); (d) photomicrograph of sample LP-15-1 with micro-bone fragment (b), burnt clay aggregate (bc), and rock fragment (rf) (PPL); (e) photomicrograph of sample LP-15-2 with micro-bone fragment (b) in the spongy microstructure (PPL); (f) sample LP-15-3 with micro-bone fragment (b) and rock fragments (rf) (PPL). PPL, plane-polarized light [Color figure can be viewed at wileyonlinelibrary.com]

the resolution (all spectra in our study contain 1800 intensity measurements). PCA is a mathematical model of data reduction that classifies multidimensional data sets into a coordinate system (based on the principal components) and may potentially reveal clusters (J. N. Miller & Miller, 2010). It is a powerful tool to infer patterns and relationships, and to explain the variations within complex series of data. In this study, PCA was used to explain the variations within the three sets of archaeological samples, and to determine if there is any relationship between spectral variance and the presence or absence of carbonate hydroxyapatite in the sediments. Although this evaluation could be done visually, PCA allows for the rapid classification of large quantities of samples (e.g., the more than 80 infrared spectra processed in this study).

3 | RESULTS AND DISCUSSION

3.1 | FTIR and second derivative spectra of archaeological samples

Three main mineral components can be identified in the FTIR spectra between 4000 and 450 cm⁻¹ produced by all archaeological samples, also present in the natural soil near the MC site (SOIL1): quartz; kaolinite; and montmorillonite (Figure 3a) (see the Supporting Information Material for the raw data of each spectra from CH, LP, MC, and the soil references). All archaeological samples show peaks at ~1090, ~1035, ~914, ~796, ~781, ~695, ~645, ~535, and ~512 cm⁻¹. These peaks correspond to clay

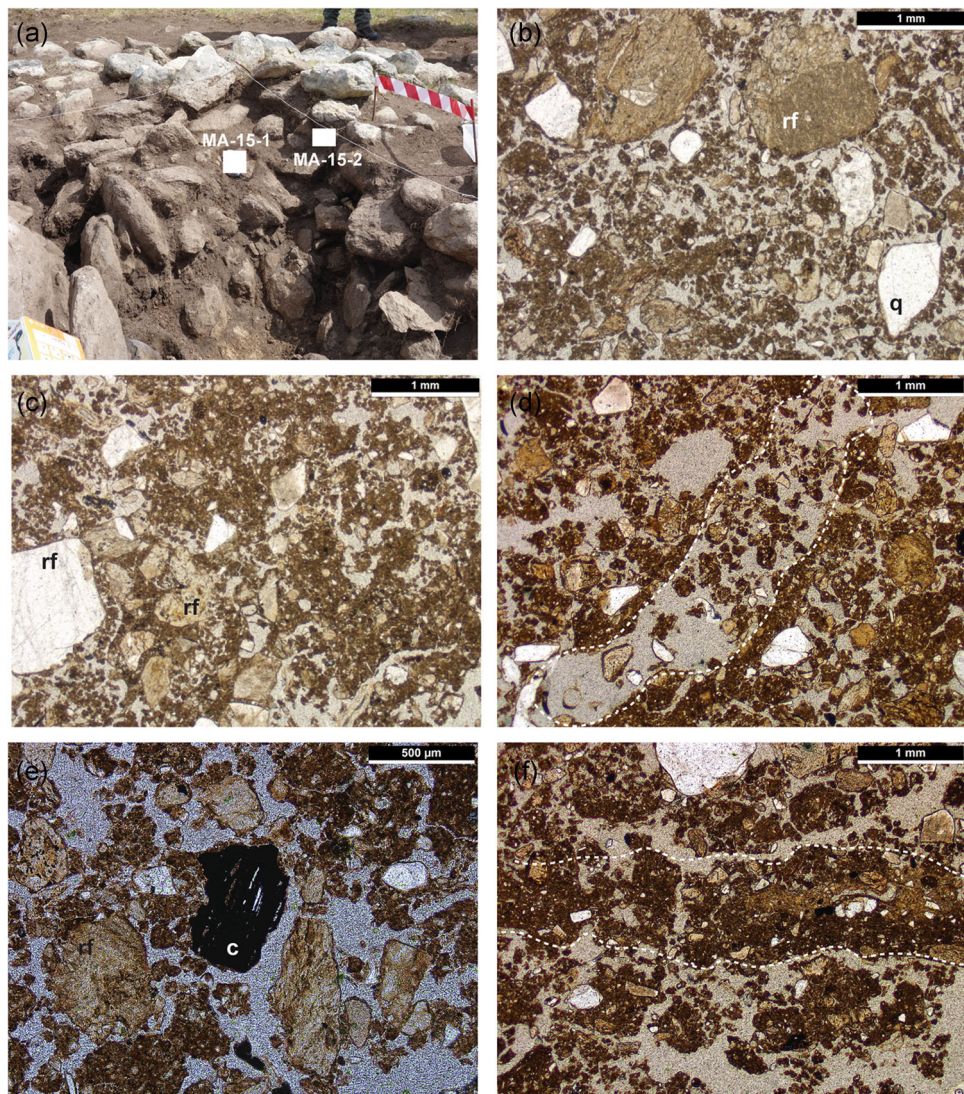


FIGURE 6 Micromorphology from the Mario Chafalote (MC) cairn. (a) Profile of M with the location of two micromorphology blocks; (b) photomicrograph of sample MA-15-1 with rock fragments (rf) and quartz (q) (PPL); (c) photomicrograph of sample MA-15-2 with rock fragments (rf) (PPL); (d) photomicrograph of sample MA-15-1 with fauna channel with excrements; (e) sample MA-15-1 with charcoal (c); and (f) surface crust in sample MA-15-1. PPL, plane-polarized light [Color figure can be viewed at wileyonlinelibrary.com]

minerals, quartz, and plagioclase. Clay minerals are identified by the peaks at the OH stretching area of the spectra (between ~ 3700 and 3600 cm^{-1}), a dominant peak at ~ 1035 , corresponding to the Si-O-Si stretching band, and the secondary peaks at $\sim 914\text{ cm}^{-1}$ (Al-O-H) and $\sim 535\text{ cm}^{-1}$ (Si-O-Al) (Beauvais & Bertaux, 2002; Madejova & Bujd, 1996; Ritz et al., 2010). The doublet at ~ 796 , ~ 781 could correspond to clay and/or quartz; the latter is also identified by the shoulder at $\sim 1090\text{ cm}^{-1}$, and the single peak at $\sim 695\text{ cm}^{-1}$ (Lippincott et al., 1958; Razva et al., 2014). The shoulder at $\sim 580\text{ cm}^{-1}$ is assigned to plagioclase.

Figure 3b shows selected spectra from each site for comparison. The CH1 sample shows the $v_4\text{PO}_4$ peaks at 602 and 566 cm^{-1} of carbonate hydroxyapatite, which are absent from the LP1 and MC1 samples that show the closest resemblance to the soil (SO1). Measurements of pH at the CH site indicated an alkaline environment

(8.3) favoring bone preservation, with acidic pH only at the topmost layer (6.3). LP has pH values between 6.5 and 5.3, and one sample from MC showed an acidic pH of 4.9, favoring bone dissolution.

Only in samples from CH (CH1, CH3, CH4, CH7, CH9) do the $v_4\text{PO}_4$ peaks at ~ 604 and $\sim 565\text{ cm}^{-1}$ appear together with a peak at $\sim 634\text{ cm}^{-1}$, corresponding to the hydroxyl peak of hydroxyapatite (Figure 3b). This means that hydroxyapatite is present in the sediments from CH, despite soil acidity (pH ranges from 6.3 to 8.1 in samples CH1 to CH9). One sample from CH also showed a calcite peak at $\sim 710\text{ cm}^{-1}$.

In the second derivative spectra in which the underlying bands become visible, samples from CH also reveal the $v_4\text{PO}_4$ bands and the OH peak of hydroxyapatite, while samples from LP and MC do not (Figure 3c,d). This could be due to the complete absence of bone mineral in samples from LP and MC.

Other phosphate minerals that could have recrystallized from the combination of leached clay iron and/or aluminum and dissolving bone mineral in low pH, such as crandallite, montgomeryite, or taranakite, were not detected in the FTIR-KBr spectra. These minerals have diagnostic peaks in the spectral range between 700 and 500 cm^{-1} (Chukanov, 2014; C. E. Miller et al., 2016).

The consistent presence of carbonate hydroxyapatite with the peak at $\sim 634 \text{ cm}^{-1}$ in the sediments from CH indicates that bones burnt at high temperatures (above 500°C) are in the sediments (Berna et al., 2012; Snoeck et al., 2014; Stiner et al., 1995; Thompson et al., 2009, 2013). This has been reported by previous zooarchaeological studies in mound A, excavation IA. Moreno (2014) reported thermal alteration in about 30% of the deer bones analyzed at the CH site (among which, ca. 50% were calcined), and also in fish bones, guinea-pigs, rodents, armadillos, birds, reptiles, and ñandu egg fragments (*Rhea americana*). About 50% of undetermined bone remains showed signs of heating, most of them calcined (Moreno, 2014). Bica (2020) showed that about 7.5% of the fish bones analyzed from the CH site show various degrees of heating.

The presence of calcite in the sediments from CH is also consistent with observations made by Moreno (2014, 2017), who identified the precipitation of calcium carbonates in bones from the CH site, sometimes reaching almost 50% of the faunal assemblage in some stratigraphic layers (about 25% of the 4576 bones analyzed at the site). Physical fragmentation of the animal bones at CH is also a common phenomenon, affecting 94% of the remains analyzed by Moreno (2014, 2017). Highly fragmented and heated bones could be contributing to the presence of hydroxyapatite in the CH sediments.

3.2 | XRPD

The variable concentrations of hydroxyapatite described for CH samples by FTIR were also identified in XRPD analyses (e.g., CH3, CH4, CH7, and CH9) (Figure 4a). XRPD analyses in selected samples from MC and LP indicate the absence of bone mineral and hydroxyapatite in the sediments within the experimental error of the technique (Figure 4b,c). Only the MC samples have weak signals in the region 30–35° that do not match the reflections of bone mineral (intense reflection at 31.8° (100), 32.18° (72), and others between 31 and 34°). LP samples have no signal in this region. Thus, XRPD measurements confirm the absence of bone mineral in the samples from MC and LP, as indicated in the FTIR data.

3.3 | Micromorphology

Micromorphological analyses of MC and LP showed typical characteristics of A horizons, such as granular, channel-vughy, or spongy microstructures; numerous channel and chamber voids; and passage features (Figure 6d). In LP, the fine fraction is dark brown, with undifferentiated b-fabric made of clay and organic matter (Figure 5b–f). In MC, the fine fraction is brown, containing more clay than organic

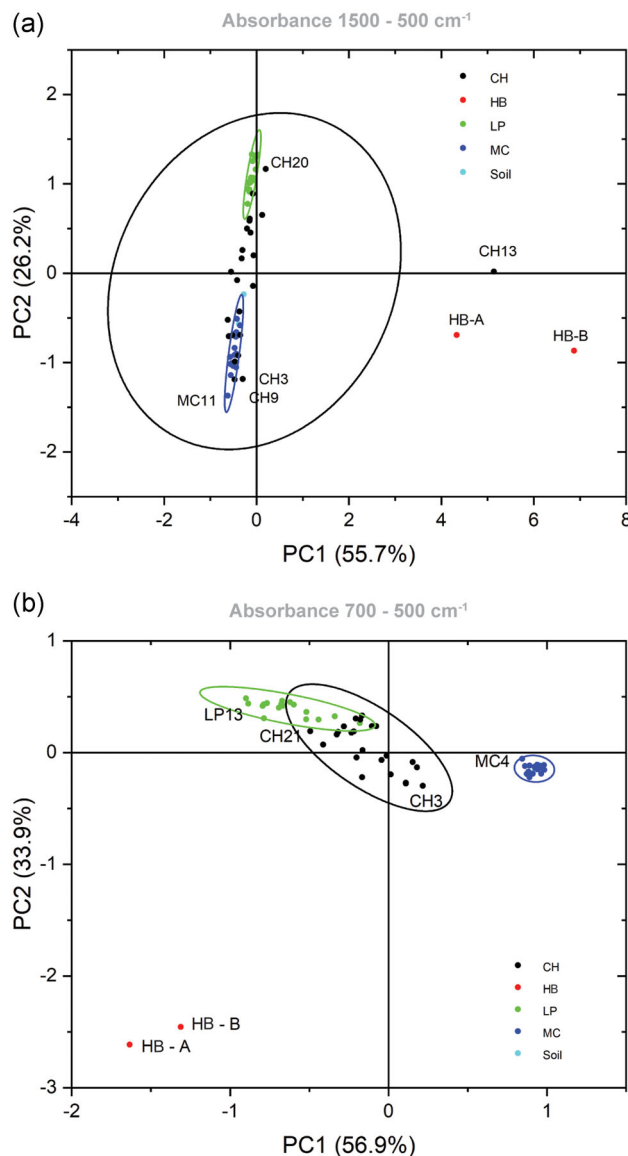


FIGURE 7 Multivariate statistics of the absorbance spectra from archaeological and reference samples (soil and bone–HB). (a) Principal component analysis (PCA) score plot for the first two principal components of the normalized absorbance spectra between 1500 and 500 cm^{-1} of archaeological samples (from sites CH, LP, and MC), natural soil, and bone mineral (HB-A and HB-B). Archaeological samples form overlapping clusters in the center of the score plot. (b) PCA score plot for the first two principal components of the normalized absorbance spectra between 700 and 500 cm^{-1} . Note how the same samples form three distinct groups. CH, CH2D01; LP, Las Palmas mound; MC, Mario Chafalote cairn [Color figure can be viewed at wileyonlinelibrary.com]

matter (Figure 6b–f). MC sediments contain a millimetric fragment of a dislocated surface crust (Figure 6f). In both sites, the coarse fraction contains angular to subangular quartz grains and local rock fragments. Rock fragments are more abundant in the sediments from MC (Figure 6b,c), while LP has a higher frequency of quartz grains (Figure 5b,c).

A single fragment of charcoal (500 μm) was identified in one sample from MC (Figure 6e), but no other anthropogenic

TABLE 2 Cumulative percentages of the correlation matrix for principal components 1 to 10 (PC1–PC10) of archaeological samples from CH, LP, and MC

	Absorbance spectra		Second derivative	
	1500–500 cm ⁻¹ 7A	700–500 cm ⁻¹ 7B	1500–500 cm ⁻¹ 7C	700–500 cm ⁻¹ 7D
PC1	55.7	56.8	69.6	80.8
PC2	81.9	90.8	86.5	92.9
PC3	92.6	98.0	93.6	95.1
PC4	96.4	98.8	95.7	96.8
PC5	98.8	99.2	97.2	98.3
PC6	98.9	99.5	97.9	98.8
PC7	99.5	99.6	98.4	99.1
PC8	99.6	99.7	98.7	99.4
PC9	99.7	99.8	99.0	99.6
PC10	99.8	99.9	99.2	99.8

Note: Cumulative percentages are given both for the absorbance and second derivative spectra in the spectral ranges between 1500–500 cm⁻¹ and 700–500 cm⁻¹.

Abbreviations: CH, CH2D01; LP, Las Palmas; MC, Mario Chafalote.

components were described in the thin sections. Sediments from LP contain very few, 1–2 mm rounded aggregates of heated clay in the coarse fraction (<1%) (Figure 5b,c). The identification of heating in these aggregates was confirmed by previous FTIR-Attenuated Total Reflectance analyses. Only sample LP-16-2 (~20–30 cm deep) contains a micro-flake and a pottery fragment. Very few dispersed micro-fragments of charcoal (≤500 µm) and bone (≤300 µm) are described in the four samples from LP, but in concentrations below 1% in the thin sections (Figure 5d–f). All the micro-bone fragments display sharp edges and show no signs of dissolution at high magnifications.

Micromorphology revealed that bone fragments in LP are in such low concentrations that they were not detected in the FTIR and XRPD analyses (between 1 and 5 micro-fragments per slide). In MC, no micro-bones were described and this, coupled with the FTIR results showing no traces of bone mineral, confirms the absence of bones in the deposit. Unfortunately, no micromorphology samples are available CH, the only site with macroscopic bone fragments and hydroxyapatite in the FTIR measurements. No other macroscopic sources of phosphates have been reported for the analyzed sites (e.g., coprolites or other fecal material, plant remains) or identified in the thin sections.

3.4 | Multivariate analysis

To investigate the relation between our three sets of archaeological samples (CH, LP, and MC), we applied a PCA model to the normalized absorbance spectra in the 1500–500 cm⁻¹ range. We plotted the archaeological samples together with our references for natural soil and bone mineral. The bone samples correspond to fragments from a

human humerus and maxilla recovered from an archaeological site nearby (Table 1). The maxilla (HB-B) shows diagenetic precipitation of calcite in the FTIR spectra (peak at ~710 cm⁻¹–v₄CO₃). For the first two components, no major differences were revealed between the samples from CH, LP, and MC, which formed one overlapped cluster in the center of the score plot with two outliers corresponding to our references for bone mineral (HB-A and HB-B), and a sample from CH containing calcite (Figure 7a).

To remove areas of irrelevant variation, we applied the PCA model to the spectra between 700 and 500 cm⁻¹, which comprise the v₄PO₄ bending vibration bands of phosphates. Here, three discrete groups were revealed for the first and second components, explaining 90.8% of the variance (Figure 7b; Table 2). The three well-differentiated groups are as follows: (1) samples from CH at the center of the score plot, with higher proximity to bone, corroborating the presence of bone mineral in some of the samples, as indicated by FTIR and XRPD; (2) samples from LP, with higher proximity to samples from CH; and (3) samples from MC, which group with the natural soil and deviate from the CH, LP, and bone mineral samples (Figure 7b).

When using the PCA model in the second derivative spectra between 1500 and 500 cm⁻¹, the same three discrete clusters are revealed for the first and second components, which explain 86% of the variance (Figure 8a; Table 2). The soil samples cluster with the sediments from MC and samples from CH group closer to the bone references (sample CH13 is closest to the bone references because of its calcite content). This means that samples can be grouped and classified when using the PCA model in a wider spectral range of the second derivative.

The PCA model of the second derivative spectra between 700 and 500 cm⁻¹ shows the same three clusters, and here, the first two components explain 92.9% of the variance (Figure 8b; Table 2). Samples from the MC cluster with the soil samples and separate from

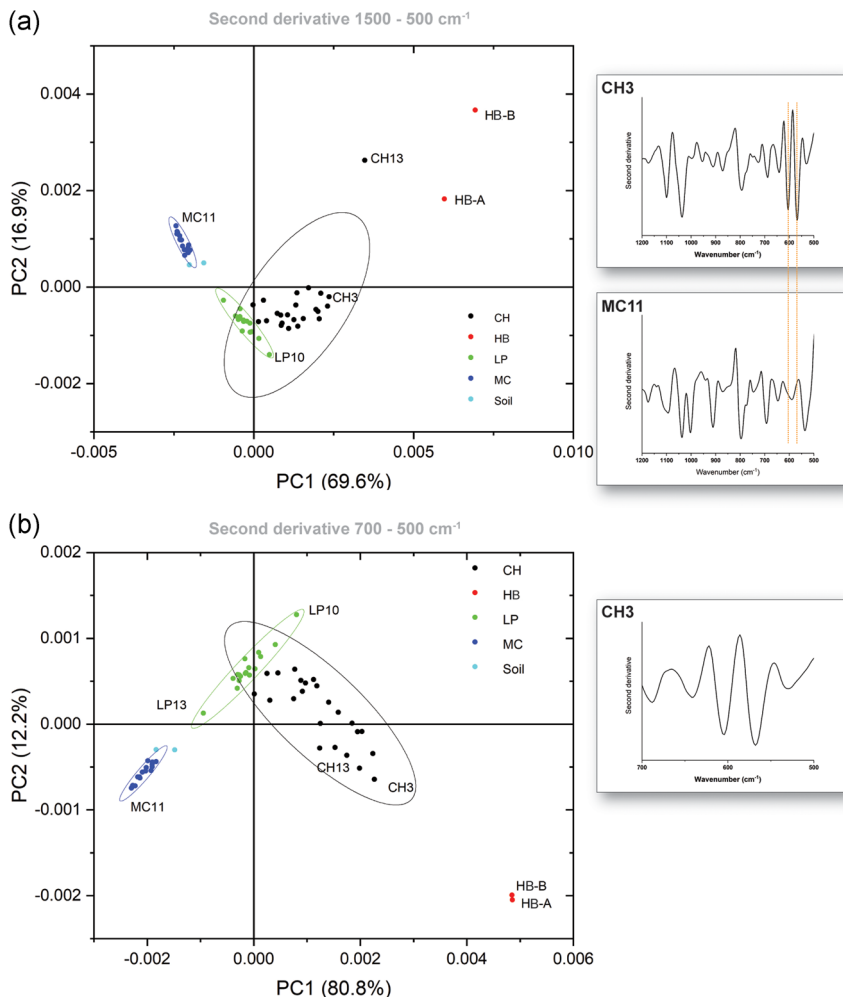


FIGURE 8 Multivariate statistics of the second derivative spectra from archaeological and reference samples. (a) Principal component analysis (PCA) score plot for the first two principal components of the second derivative spectra between 1500 and 500 cm^{-1} of archaeological samples (CH, LP, and MC), natural soil, and the bone references (HB). The archaeological samples form three discrete clusters, with partial overlapping between the CH and LP samples. Details of the second derivative spectra between 1200 and 500 cm^{-1} for sample CH3, with the two minima corresponding to the 604 and 565 cm^{-1} phosphate vibration bands, and sample MC11, without any indication of phosphates. (b) PCA score plot for the first two principal components of the second derivative spectra between 700 and 500 cm^{-1} . Details of the second derivative spectra between 700 and 500 cm^{-1} for sample CH3, containing hydroxyapatite. CH, CH2D01; LP, Las Palmas mound; MC, Mario Chafalote cairn [Color figure can be viewed at wileyonlinelibrary.com]

LP and CH. CH displays a wider dispersion, with some samples closer to the bone reference, due to the presence of the $\nu_4\text{PO}_4$ bending vibration bands of phosphates.

The PCA model suggests that, while some of the samples from CH display the $\nu_4\text{PO}_4$ bending vibration bands of phosphates, others do not and group with LP and MC. The narrower the spectral range for the second derivative (Figure 8b), the more separated the clusters become, pointing to a variance explained by the $\nu_4\text{PO}_4$ peaks, for the CH samples, and by other bands in the spectrum, for LP and MC. The PCA results confirm that neither the LP nor MC samples have detectable amounts of bone mineral and that differences between them, at least in the 700–500 cm^{-1} range, are due to other minerals.

4 | CONCLUSION

Earthen mounds containing low amounts of bones have challenged the traditional model for earthen mound construction in the Uruguayan lowlands, which refers to the reworking of faunal remains and other domestic refuse. Bone dissolution in acidic soils has been the most common explanation to account for the absence of bones in

several earthen mounds. In this study, we applied for the first time the inexpensive and rapid technique of FTIR spectrometry, coupled with XRPD and micromorphology, to investigate the presence of bone remains in three archaeological sites of Eastern Uruguay located in similar environmental conditions. Our premise is that phosphates may still be present in the soil after dissolution of the bone mineral and be detectable by FTIR, XRPD, and micromorphology.

FTIR analyses show hydroxyapatite exclusively in samples from the CH mound, indicating the presence of burnt bones in the sediments, as has been shown by previous zooarchaeological studies (Bica, 2020; Moreno, 2014). The samples containing hydroxyapatite come from the upper layers of the site, dated between 1830–1389 and 232–124 cal B.P. At the LP site, hardly any macroscopic bones were recovered in the excavation, and neither FTIR nor XRPD revealed traces of bone mineral or other phosphates. The same situation was reported for the MC site, indicating that bones were never deposited at the sites.

Micromorphology confirmed that bone mineral or other recrystallized phosphates are completely absent from MC, but revealed very few (less than 1%) micro-bone fragments in LP whose concentration is below the detection limit of FTIR (and XRPD). Unfortunately, no micromorphology samples were available for the CH

site, which was excavated in the 1990s and no longer exists. The PCA model once again confirmed that some CH samples show the $\nu_4\text{PO}_4$ bending vibration bands of phosphates, grouping them closer to the bone reference, while samples from LP and MC do not, and group with natural soils.

Our study shows that samples from the LP mound and the MC cairn are intrinsically different from the CH mound, and do not contain any detectable traces of bone mineral or burnt bone. The compositional differences between the CH and LP earthen mounds do not result from taphonomic processes, such as intense bone dissolution in corrosive environments. Macroscopic bone fragments are abundant in the CH site and this, together with the noticeable presence of burnt bones in the sediments (see Bica, 2020; Moreno, 2014), confirms the use of domestic waste as the primary material for mound construction.

The very few bone fragments seen in the thin sections from LP were not detected by FTIR and do not derive from large amounts of bones that ultimately dissolved, despite the low pH reported for local soils. This points to different uses and building processes for both anthropogenic structures (e.g., CH and LP mounds), despite their proximity, close chronology, and cultural affinity. The ubiquitous heated clay aggregates described in the thin sections from LP could be signaling a different history for this site. Heated clay aggregates are present from the base to the top of the mound, while pottery only appears in the upper layers of LP, about 500 years ago (thermoluminescence age). Heated clay aggregates have also been described in the sediments from CH and La Tapera sites (del Puerto et al. 2021), indicating the potential use of these hard, coarse aggregates as building material for the mounds.

Earthen mounds with very low amounts of bone remains are common in the Uruguayan lowlands (e.g., Pago Lindo, Lemos PR14D01, Rubio, Cañada de los Caponcitos) (Cabrera & Marozzi, 2001; Gianotti, 2005; Gianotti et al., 2013; Villagran & Gianotti, 2013), and could be the result of mound technologies where coarse-sized domestic residues (e.g., bones, charcoal) are not used as prime material for mound building. Mounds could result from the preparation of special deposits for horticulture (e.g., elevated gardens), with high porosity and granular textures produced after reworking of surface A horizons, rich in organic matter (Gianotti, 2015, 2021). Another possibility could be related to the construction of mounds for specific activities using local soils, whose surfaces were regularly cleaned out of organic waste. The regular cleaning of a surface removes most macro and even microscopic components from the sediments (Milek, 2012). At the Los Ajos site, Iriarte (2003) interpreted the regular cleaning of specific occupation surfaces inside the excavated mounds. This was also suggested for the Pago Lindo earthen mound complex (Gazzán, 2018; Villagran & Gianotti, 2013), located in a similar environment in central-eastern Uruguay, where microscopic bones are absent and macroscopic bones are rare in sedimentary matrices made of reworked A horizons. Several lines of evidence point to multiple uses and life histories for the earthen mounds, through the active management of domestic waste and natural soils, which are possible within the context of

community-based villages that built hundreds of earthworks in the Uruguayan lowlands (Gianotti, 2015; Iriarte, 2003).

In the case of the MC cairn, the absence of any indication of macroscopic and/or microscopic bone remains, plus no detectable bone mineral, hydroxyapatite, or other secondary phosphates, contradicts historic sources suggesting that cairns were used to bury tribal chiefs. Other uses, such as points of observation or a location to make fire signals, may be attributed to this specific site, and more excavations are needed to test the hypothesis raised by ethnographic sources.

Future studies should focus on understanding the chemistry of local soils and its effects on the preservation of archaeological materials. The revelation of micro-bone fragments at LP, whose concentration was not detected by FTIR or XRD analyses, points to the need to establish the detection limit of bone mineral in FTIR measurements of complex spectra. Quantifying the detection limit of bone mineral in FTIR measurements could potentially be used to estimate the amount of weathered bone that can contribute to detectable bone mineral in archaeological sediments and soils.

ACKNOWLEDGMENTS

The authors would like to thank Francesco Berna for providing helpful comments on an earlier version of this manuscript. Thanks are due to the CRALM research team under the coordination of Profs. J. M. Lopez Mazz and R. Bracco, who conducted excavations at CH2D01. The research team of the Laboratorio de Arqueología del Paisaje y Patrimonio del Uruguay (LAPPU, FHCE) excavated and sampled Las Palmas and Mario Chafalote. Samples were processed and analyzed at the Laboratório de Alto Impacto—Centro Universitário Regional do Este (CURE), guided by Dr. Laura Fornero. Thanks are due to Paulina Abre (CURE, Treinta y Tres) for providing the reference samples for local minerals. Micro-morphological analyses were performed at the Laboratory of Microarchaeology of the University of São Paulo. Funding for this study was provided by the Comisión Sectorial para la Investigación Científica (CSIC I + D grants 2015-2017/94, and 2017-2019/ 338) and the Fundação de Amparo à Pesquisa do Estado de São Paulo (FAPESP, grant 2015/19405-6).

ORCID

Ximena S. Villagran  <http://orcid.org/0000-0001-8630-2015>

Mauricio Rodriguez  <http://orcid.org/0000-0002-9890-0933>

Heinkel Bentos Pereira  <http://orcid.org/0000-0002-1912-9520>

Camila Gianotti  <http://orcid.org/0000-0002-1446-3503>

Moira Sotelo  <http://orcid.org/0000-0001-8156-0963>

Laura del Puerto  <http://orcid.org/0000-0003-2003-9263>

REFERENCES

Aragão, B. J. G. de, & Messaddeq, Y. (2008). Peak separation by derivative spectroscopy applied to ftir analysis of hydrolyzed silica. *Journal of the Brazilian Chemical Society*, 19, 1582–1594.

Beauvais, A., & Bertaux, J. (2002). In situ characterization and differentiation of kaolinites in lateritic weathering profiles using infrared microspectroscopy. *Clays and Clay Minerals*, 50(3), 314–330. <https://doi.org/10.1346/00098600260358076>

Berna, F., Goldberg, P., Horwitz, L. K., Brink, J., Holt, S., Bamford, M., & Chazan, M. (2012). Microstratigraphic evidence of in situ fire in the Acheulean strata of Wonderwerk Cave, Northern Cape province, South Africa. *Proceedings of the National Academy of Sciences of the United States of America*, 109(20), E1215–E1220. <https://doi.org/10.1073/pnas.1117620109>

Berna, F., Matthews, A., & Weiner, S. (2004). Solubilities of bone mineral from archaeological sites: The recrystallization window. *Journal of Archaeological Science*, 31(7), 867–882. <https://doi.org/10.1016/j.jas.2003.12.003>

Bica, C. (2020). *Peces y pesca en las tierras bajas de la Laguna Merín. Análisis de la ictiofauna recuperada en el sitio arqueológico CH2D01 (Rocha, Uruguay)*. Universidad Federal de Pelotas.

Bracco, R. (2006). Montículos de la Cuenca de la Laguna Merín: Tiempo, Espacio y Sociedad. *American Antiquity*, 17(4), 511–540.

Bracco, R., Cabrera, L., & Lopez Mazz, J. (2000). La Prehistoria de las Tierras Bajas de la Cuenca de la Laguna Merín. In A. Duran & R. Bracco (Eds.), *Arqueología de las Tierras Bajas* (pp. 13–38). Imprenta Americana.

Bracco, R., Inda, H., & del Puerto, L. (2015). Complejidad en montículos de la cuenca de la Laguna Merín y análisis de redes sociales. *Intersecciones En Antropología*, 16, 271–286.

Cabrera, L. (2005). Patrimonio y Arqueología en el Sur de Brasil y región Este del Uruguay: los cerritos de indios. *Saldvie*, 5, 221–254.

Cabrera, L., & Marozzi, O. (2001). Sitio PR14D01, Río Tacuari, Depto. de Treinta y Tres. In: Arqueología uruguaya hacia el fin del milenio. IX Congreso de Arqueología Uruguaya (pp. 69–82). MEC, Fundación Fontaina-Minelli y AUA. Montevideo: Gráficos del Sur.

Capdepont, I., del Puerto, L., & Inda, H. (2005). Instrumentos de molienda: evidencias del procesamiento de recursos vegetales en la laguna de Castillos (Rocha, Uruguay). *Intersecciones En Antropología*, 6, 153–166.

Capdepont, I., & Pintos, S. (2006). Manejo y aprovechamiento del medio por parte de los grupos constructores de montículos: cuenca de la Laguna de Castillos, Rocha–Uruguay. *Relaciones de La Sociedad Argentina de Antropología*, XXXI, 117–132.

Chukanov, N. V. (2014). *Infrared spectra of mineral species*. Springer.

Collins, M. J., Nielsen-Marsh, C. M., Hiller, J., Smith, C. I., Roberts, J. P., Prigodich, R. V., Wess, T. J., Csapo, J., Millard, A. R., & Turner-Walker, G. (2002). The survival of organic matter in bone: A review. *Archaeometry*, 44(3), 383–394. <https://doi.org/10.1111/1475-4754.t01-1-00071>

Curbelo, C., Bracco, R., Cabrera, L., Femenias, N., Fusco, N., Lopez Mazz, J., & Martinez, E. (1990). Estructuras de sitio y zonas de actividad: sitio CH2D01, área de San Miguel, Departamento de Rocha. *ROU. Revista Do CEPA*, 17(20), 333–344.

Dal Sasso, G., Lebon, M., Angelini, I., Maritan, L., Usai, D., & Artioli, G. (2016). Bone diagenesis variability among multiple burial phases at Al Khiday (Sudan) investigated by ATR-FTIR spectroscopy. *Palaeogeography, Palaeoclimatology, Palaeoecology*, 463, 168–179. <https://doi.org/10.1016/j.palaeo.2016.10.005>

del Puerto, L., Gianotti, C., Bortolotto, N., Gazzán, N., Canela, C., Orrego, B., & Inda, H. (2021). Geoarchaeological signatures of anthropogenic soils in southeastern Uruguay: Approaches to formation processes and spatial-temporal variability. *Gearchaeology*, 37, 180–197. <https://doi.org/10.1002/gea.21854>

Femenias, J. (1983). Amontonamientos artificiales de piedras en cerros y elevaciones de nuestro territorio. *Revista Antropológica*, 1(1), 13–16.

Femenias, J., Lopez-Mazz, J., Bracco, R., Cabrera, L., Curbelo, C., Fusco, N., & Martinez, E. (1990). Tipos de Enterramiento en estructuras monticulares cerritos, en la región de la cuenca de la Laguna Merín. *ROU. Revista Do CEPA*, 17(20), 345–356.

Figueira, J. J. (1958). *Una excursión arqueológica al Cerro Tupambay realizada en los comienzos de 1881. Separata de la Revista Nacional. Ministério de Instrucción Pública*.

Figueira, J. J. (1965). Brevario de Etnografía y Arqueología del Uruguay. *Boletín Histórico Del Estado Mayor General Del Ejército*, 104, 29–68.

Friesem, D. E., Lavi, N., Madella, M., Ajithprasad, P., & French, C. (2016). Site formation processes and hunter-gatherers use of space in a tropical environment: A geo-ethnoarchaeological approach from South India. *PLoS One*, 11(10), e0164185. <https://doi.org/10.1371/journal.pone.0164185>

Gazzán, N. (2018). *Analís de la distribución especial del material lítico del sitio Pago Lindo (Caraguatá, Departamento de Tacuarembó)*. Tesis de Maestría. Departamento de Arqueología, Fac. De Humanidades y Ciencias de la Educación.

Gianotti, C. (2005). Intervenciones arqueológicas en el cerrito 27 del Conjunto Lemos. *TAPA*, 36, 79–98.

Gianotti, C. (2015). *Paisajes Sociales, Monumentalidad y Territorio en las Tierras Bajas de Uruguay* [PhD degree thesis, 711 pp, Facultad de Xeografía e Historia, Universidad de Santiago de Compostela].

Gianotti, C. (2021). Environment transformation and landscape domestication in the lowlands of Northeast of Uruguay. Earthworks as technology for the management of flood ecosystems. In M. Bonomi & S. Archila (Eds.), *South American contributions to world archaeology* (pp. 283–316). Springer Nature.

Gianotti, C., del Puerto, L., Inda, H., & Capdepont, I. (2013). Construir para producir. Pequeñas elevaciones en tierra para el cultivo del maíz en el sitio Cañada de los Caponcitos, Tacuarembó (Uruguay). *Cuadernos del Instituto Nacional de Antropología y Pensamiento Latinoamericano*, 1(1), 12–25.

Gianotti, C., & Lopez-Mazz, J. (2009). Prácticas mortuorias en la localidad arqueológica Rincón de los Indios, Departamento de Rocha. In J. Lopez-Mazz & A. Gascue (Eds.), *Arqueología Prehistórica Uruguaya en el Siglo* (Vol. XXI, pp. 151–196). Biblioteca Nacional.

Hedges, R. E. M. (2002). Bone diagenesis: An overview of processes. *Archaeometry*, 44(3), 319–328. <https://doi.org/10.1111/1475-4754.00064>

Iriarte, J. (2003). *Mid-Holocene emergent complexity and landscape transformation: The social construction of early formative communities in Uruguay, La Plata Basin* [Doctor degree thesis of College of Arts and Science, University of Kentucky, Lexington].

Iriarte, J. (2006). Landscape transformation, mounded villages and adopted cultigens: The rise of early Formative communities in south-eastern Uruguay. *World Archaeology*, 38(4), 644–663.

Jans, M. (2004). Characterisation of microbial attack on archaeological bone. *Journal of Archaeological Science*, 31(1), 87–95. <https://doi.org/10.1016/j.jas.2003.07.007>

Karkanas, P. (2000). Diagenesis in Prehistoric Caves: the Use of Minerals that Form In Situ to Assess the Completeness of the Archaeological Record. *Journal of Archaeological Science*, 27(10), 915–929. <https://doi.org/10.1006/jasc.1999.0506>

Karkanas, P. (2010). Preservation of anthropogenic materials under different geochemical processes: A mineralogical approach. *Quaternary International*, 214(1–2), 63–69. <https://doi.org/10.1016/j.quaint.2009.10.017>

Lebon, M., Reiche, I., Bahain, J. -J., Chadeaux, C., Moigne, A.-M., Fröhlich, F., Séma, F., Schwarcz, H. P., & Falguères, C. (2010). New parameters for the characterization of diagenetic alterations and heat-induced changes of fossil bone mineral using Fourier transform infrared spectrometry. *Journal of Archaeological Science*, 37(9), 2265–2276. <https://doi.org/10.1016/j.jas.2010.03.024>

Lebon, M., Reiche, I., Fröhlich, F., Bahain, J. J., & Falguères, C. (2008). Characterization of archaeological burnt bones: Contribution of a new analytical protocol based on derivative FTIR spectroscopy and curve fitting of the v 1 v 3 PO4 domain. *Analytical and Bioanalytical Chemistry*, 392, 1479–1488. <https://doi.org/10.1007/s00216-008-2469-y>

LeGeros, R. Z., & LeGeros, J. P. (1984). Phosphate minerals in human tissues. In J. O. Nriagu & P. B. Moore (Eds.), *Phosphate minerals* (351st–385th ed.). Springer-Verlag. https://doi.org/10.1007/978-3-642-61736-2_12

Lippincott, E. R., Vanvalkenburg, A., Weir, C. E., & Bunting, E. N. (1958). Infrared studies on polymorphs of silicon dioxide and germanium dioxide. *Journal of Research of the National Bureau of Standards*, 61(1), 61. <https://doi.org/10.6028/jres.061.009>

Lopez-Mazz, J. (2001). Las estructuras tumulares (cerritos) del Litoral Atlántico uruguayo. *Latin American Antiquity*, 12(4), 231–255.

Madejova, J., & Bujd, J. (1996). Preparation and infrared spectroscopic characterization of reduced-charge montmorillonite with various Li contents. *Mineralogical Society*, 31, 233–241.

Milek, K. B. (2012). Floor formation processes and the interpretation of site activity areas: An ethnoarchaeological study of turf buildings at Thverá, northeast Iceland. *Journal of Anthropological Archaeology*, 31(2), 119–137. <https://doi.org/10.1016/j.jaa.2011.11.001>

Miller, C. E., Goldberg, P., & Berna, F. (2013). Geoarchaeological investigations at Diepkloof Rock Shelter, Western Cape, South Africa. *Journal of Archaeological Science*, 40(9), 3432–3452. <https://doi.org/10.1016/j.jas.2013.02.014>

Miller, C. E., Mentzer, S. M., Berthold, C., Leach, P., Ligouis, B., Tribolo, C., & Porraz, G. (2016). Site-formation processes at Elands Bay Cave, South Africa. *African Humanities*, 29, 69–128.

Miller, J. N., & Miller, J. C. (2010). *Statistics and chemometrics for analytical chemistry*. Pearson Education Limited.

Monnier, G. F. (2018). A review of infrared spectroscopy in microarchaeology: Methods, applications, and recent trends. *Journal of Archaeological Science: Reports*, 18, 806–823. <https://doi.org/10.1016/j.jasrep.2017.12.029>

Moreno, F. (2014). *La gestión de los recursos animales en la prehistoria del Este de Uruguay (4000 años AP–Sigo XVI)*. Universitat Autònoma de Barcelona

Moreno, F. (2016). La gestión animal en la prehistoria del Este de Uruguay: de la economía de amplio espectro al control de animales salvajes. *Tessituras*, 4(1), 161–187.

Moreno, F. (2017). Modificaciones naturales y antrópicas en el conjunto zooarqueológico del sitio CH2D01, Excavación IA (Sudeste uruguayo): aportes a la discusión de los procesos de formación. *Cadernos Do LEPAARQ*, 14, 458–479.

Moreno, F., Figueira, G., & Sans, M. (2014). Huesos mezclados: restos humanos de subadultos en el conjunto arqueofaunístico de un sitio prehistórico en el este de Uruguay. *Revista Argentina de Antropología Biológica*, 16(2), 65–78.

Nielsen-Marsh, C. M., & Hedges, R. E. (2000). Patterns of diagenesis in bone I: The effects of site environments. *Journal of Archaeological Science*, 27(12), 1139–1150. <https://doi.org/10.1006/jasc.1999.0537>

Nielsen-Marsh, C. M., Smith, C., Jans, M., Nord, A., Kars, H., & Collins, M. (2007). Bone diagenesis in the European Holocene II: Taphonomic and environmental considerations. *Journal of Archaeological Science*, 34(9), 1523–1531. <https://doi.org/10.1016/j.jas.2006.11.012>

Nriagu, J. O., & (1976). Phosphate-clay mineral relations in soils and sediments. *Canadian Journal of Earth Sciences*, 13, 717–736.

Pintos, S. (2000). Economía “húmeda” del este de Uruguay: el manejo de recursos faunísticos. In A. Durán & R. Bracco (Eds.), *Arqueología de las Tierras Bajas* (pp. 249–270). Comisión Nacional de Arqueología, Ministerio de Educación y Cultura.

Pintos, S., & Capdepont, I. (2001). Arqueología en la Cuenca de la Laguna de Castillos. Apuntes sobre complejidad cultural en sociedades cazadoras recolectoras del Este de Uruguay. *ArqueoWeb: Revista Sobre Arqueología En Internet*, 3(2). <https://webs.ucm.es/info/arqueoweb/pdf/3-2/pintos.pdf>

Pintos, S., & Gianotti, C. (1995). Arqueofauna de los constructores de cerritos: “quebra” y requiebra. In M. Consens, J. López Mazz, & C. Curbelo (Eds.), *Arqueología en el Uruguay. VIII Congreso Nacional de Arqueología Uruguaya* (pp. 79–91). Editorial Surcos.

Portas, M., & Sans, M. (1995). Historias de vida en los restos esqueletales de dos sitios con elevación del Departamento de Rocha. In M. Consens, J. Lopez-Mazz, & C. Curbelo (Eds.), *Arqueología en el Uruguay. VIII Congreso Nacional de Arqueología Uruguaya* (pp. 22–35). Imprenta Americana.

Razva, O., Anufrienkova, A., Korovkin, M., Ananieva, L., & Abramova, R. (2014). Calculation of quartzite crystallinity index by infrared absorption spectrum. *IOP Conference Series: Earth and Environmental Science*, 21, 012006. <https://doi.org/10.1088/1755-1315/21/1/012006>

Ritz, M., Vaculíková, L., & Plevová, E. (2010). Identification of clay minerals by infrared spectroscopy and discriminant analysis. *Applied Spectroscopy*, 64(12), 1379–1387. <https://doi.org/10.1366/000370210793561592>

Sans, M., & Femenias, J. (2000). Subsistencia, Movilidad y Organización Social en el Sitio Monticular CH2D01-A (Rocha-Uruguay): Inferencias a Partir de las Pautas de Enterramientos y los Restos Esqueletarios. In A. Duran & R. Bracco (Eds.), *Arqueología de las Tierras Bajas* (pp. 385–396). Imprenta Americana.

Schiegl, S. (1996). Ash deposits in Hayonim and Kebara Caves, Israel: Macroscopic, microscopic and mineralogical observations, and their archaeological implications. *Journal of Archaeological Science*, 23(5), 763–781. <https://doi.org/10.1006/jasc.1996.0071>

Shahack-Gross, R., Bar-Yosef, O., & Weiner, S. (1997). Black-coloured bones in Hayonim cave, Israel: Differentiating between burning and oxide staining. *Journal of Archaeological Science*, 24(5), 439–446. <https://doi.org/10.1006/jasc.1996.0128>

Skinner, H. C. (2005). Mineralogy of bone. In O. Selinus (Ed.), *Essentials of medical geology: Impacts of the natural environment on public health* (pp. 667–678). Elsevier.

Smith, C., Nielsen-Marsh, C., Jans, M., & Collins, M. (2007). Bone diagenesis in the European Holocene I: Patterns and mechanisms. *Journal of Archaeological Science*, 34(9), 1485–1493. <https://doi.org/10.1016/j.jas.2006.11.006>

Snoeck, C., Lee-Thorp, J. A., & Schulting, R. J. (2014). From bone to ash: Compositional and structural changes in burned modern and archaeological bone. *Palaeogeography, Palaeoclimatology, Palaeoecology*, 416, 55–68. <https://doi.org/10.1016/j.palaeo.2014.08.002>

Sotelo, M. (2018). Stone structures in the highlands of Uruguay. *Encyclopedia of Global Archaeology*, 1–17. https://doi.org/10.1007/978-3-319-51726-1_3036-1

Squires, K. E., Thompson, T. J. U., Islam, M., & Chamberlain, A. (2011). The application of histomorphometry and Fourier transform infrared spectroscopy to the analysis of early Anglo-Saxon burned bone. *Journal of Archaeological Science*, 38(9), 2399–2409. <https://doi.org/10.1016/j.jas.2011.04.025>

Stiner, M. C., Kuhn, S., Weiner, S., & Bar-Yosef, O. (1995). Differential burning, recrystallization, and fragmentation of archaeological bone. *Journal of Archaeological Science*, 22(2), 223–237. <https://doi.org/10.1006/jasc.1995.0024>

Stiner, M. C., Khun, S. L., Bar-Yosef, O., Weiner, S., & Bar-Yosef, O. (1995). Differential burning, recrystallization and fragmentation of archaeological bone. *Journal of Archaeological Science*, 22, 223–237.

Stiner, M. C., Kuhn, S. L., Surovell, T. A., Goldberg, P., Meignen, L., Weiner, S., & Bar-Yosef, O. (2001). Bone preservation in Hayonim Cave (Israel): A macroscopic and mineralogical study. *Journal of Archaeological Science*, 28(6), 643–659. <https://doi.org/10.1006/jasc.2000.0634>

Stoops, G. (2003). *Guidelines for Analysis and Description of Soil and Regolith Thin Sections*. Soil Science Society of America, Madison.

Thompson, T. J. U., Gauthier, M., & Islam, M. (2009). The application of a new method of Fourier transform infrared spectroscopy to the analysis of burned bone. *Journal of Archaeological Science*, 36(3), 910–914. <https://doi.org/10.1016/j.jas.2008.11.013>

Thompson, T. J. U., Islam, M., & Bonniere, M. (2013). A new statistical approach for determining the crystallinity of

heat-altered bone mineral from FTIR spectra. *Journal of Archaeological Science*, 40(1), 416–422. <https://doi.org/10.1016/j.jas.2012.07.008>

Toffolo, M. B., Brink, J. S., & Berna, F. (2015). Bone diagenesis at the Florisbad spring site, Free State Province (South Africa): Implications for the taphonomy of the Middle and Late Pleistocene faunal assemblages. *Journal of Archaeological Science: Reports*, 4, 152–163. <https://doi.org/10.1016/j.jasrep.2015.09.001>

Trueman, C., Behrensmeyer, A. K., Tuross, N., & Weiner, S. (2004). Mineralogical and compositional changes in bones exposed on soil surfaces in Amboseli National Park, Kenya: Diagenetic mechanisms and the role of sediment pore fluids. *Journal of Archaeological Science*, 31(6), 721–739. <https://doi.org/10.1016/j.jas.2003.11.003>

Villagran, X. S., & Gianotti, C. (2013). Earthen mound formation in the Uruguayan lowlands (South America): Micromorphological analyses of the Pago Lindo archaeological complex. *Journal of Archaeological Science*, 40(2), 1093–1107.

Weiner, S. (2010). *Microarchaeology*. Cambridge University Press.

Weiner, S., & Bar-Yosef, O. (1990). States of preservation of bones from prehistoric sites in the Near East: A survey. *Journal of Archaeological Science*, 17(2), 187–196. [https://doi.org/10.1016/0305-4403\(90\)90058-D](https://doi.org/10.1016/0305-4403(90)90058-D)

Weiner, S., Goldberg, P., & Bar-Yosef, O. (2002). Three-dimensional distribution of minerals in the sediments of Hayonim Cave, Israel: Diagenetic processes and archaeological implications. *Journal of Archaeological Science*, 29(11), 1289–1308. <https://doi.org/10.1006/jasc.2001.0790>

Weiner, S., Schiegl, S. P. G., & Bar-Yosef, O. (1995). Mineral assemblages in Kebara and Hayonim caves, Israel: Excavation strategies, bone preservation, and wood ash remnants. *Israel Journal of Chemistry*, 35, 143–154.

SUPPORTING INFORMATION

Additional supporting information may be found in the online version of the article at the publisher's website.

How to cite this article: S. Villagran, X., Rodriguez, M., Pereira, H. B., Gianotti, C., Sotelo, M., & del Puerto, L. (2022). Absence of bones in archaeological sites from the southeast of Uruguay: Taphonomy or human behavior? *Geoarchaeology*, 37, 694–708. <https://doi.org/10.1002/gea.21906>